Supporting Information

# Helically Twining Polymerization for Constructing Polymeric Double Helix

*Huajun Huang,[a] Song Hong,[b] Junya Liang,[a] Yan Shi*[a] and Jianping Deng*[a]*

[a] State Key Laboratory of Chemical Resource Engineering, College of Materials Science and Engineering, Beijing University of Chemical Technology, Beijing 100029, China.

[b] Analysis and Test Center, Beijing University of Chemical Technology, Beijing 100029, China

## Contents

**GPC test.**

To further explore the DHSPs, we measured the molecular weights and polydispersity indices (PDIs) of P1, P2, and DHSPs by GPC (THF as eluent), as briefly summarized here: P1, Mn= 9050, PDI=1.61; P2(R), Mn=4000, PDI=1.76; P2(S), Mn=3700, PDI=1.64; *MM* DHSP, Mn=21400, PDI=1.99; *PP* DHSP, Mn=20200, PDI=2.05. The larger number-average molecular weights of DHSPs relative to those of P1 and P2 are well consistent with the formation of double helices. However, the data from GPC tests only provide a reference because the molecular models of the (double) helical polymers are quite different from polystyrenes (random coil structure) which were used as standards for the calibration of GPC tests. Moreover, the P2 prepared by general solution polymerization and by helically twining polymerization may have different molecular weights, making the above comparison slightly improper.

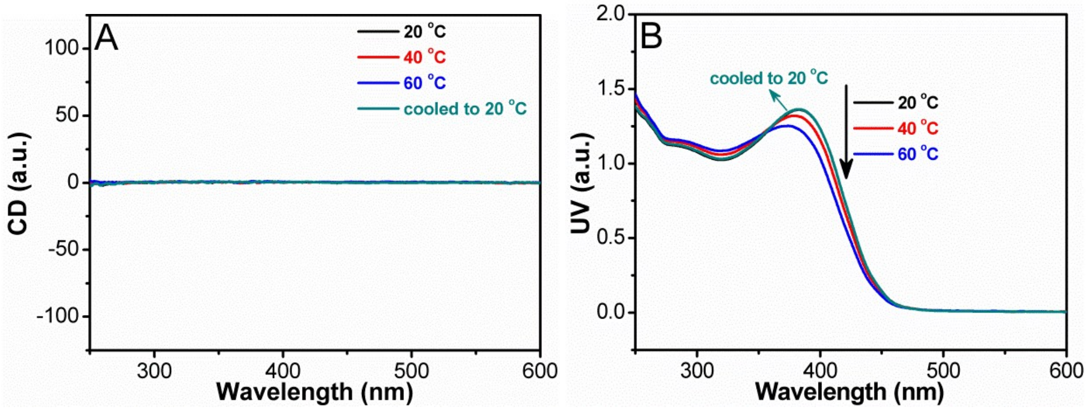

**Figure S1.** CD and UV-vis spectra of P1 dissolved in $CHCl_3$ at varied temperature: increased from 20 to 60 $^oC$ and then cooled to 20 $^oC$ again.

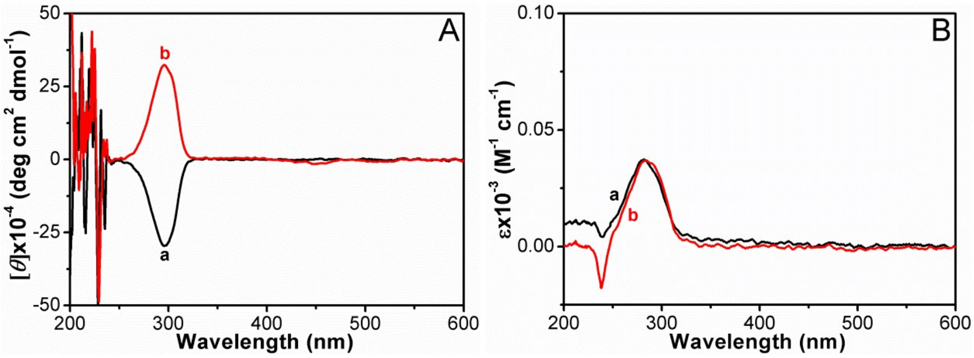

**Figure S2.** CD (A) and UV-vis (B) spectra of (a) M2(R) ($10^{-3}$ mol/L in $CHCl_3$) and (b) M2(S) ($10^{-3}$ mol/L in $CHCl_3$).

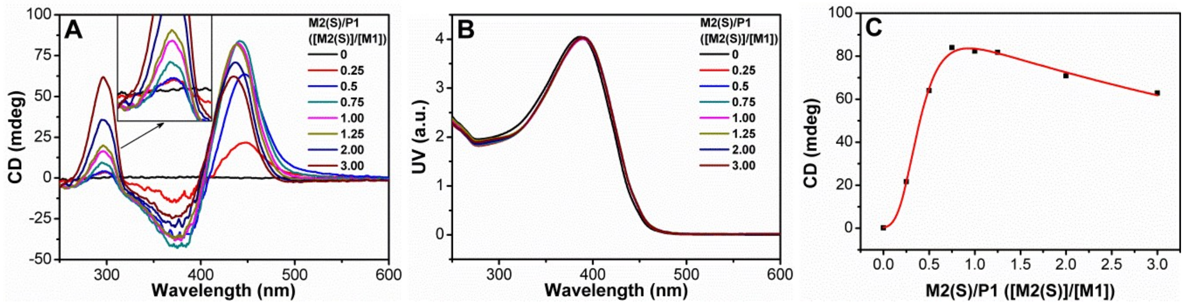

**Figure S3.** CD (A) and UV-vis (B) spectra of the solutions resulting from the chiral inductions of P1 at varied M2/P1 ([M2]/[M1]; taking M2(S) as an example). All the spectra were measured at the same P1 concentration (200 mg/L). The variation tendency of the maximum CD intensity (near 437 nm) depending on M2/P1 were drawn as red line in (C).

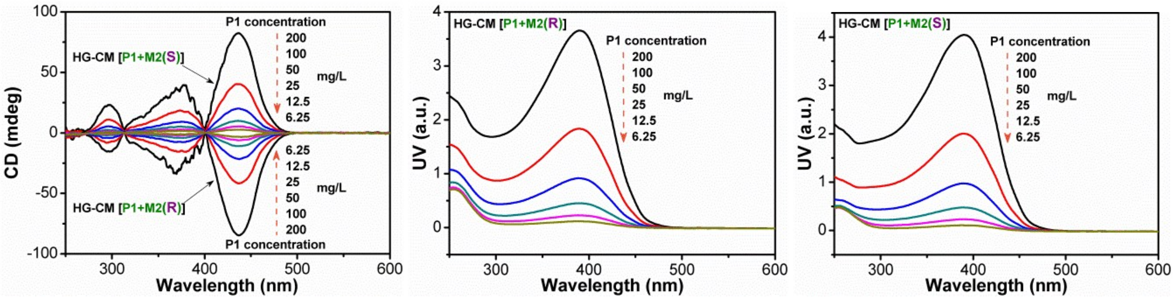

**Figure S4.** CD and UV-vis spectra of HG−CM structures in varied P1 concentrations. To perform the measurement, the solutions of HG−CM structures were diluted quantitatively to reach the predetermined P1 concentrations.

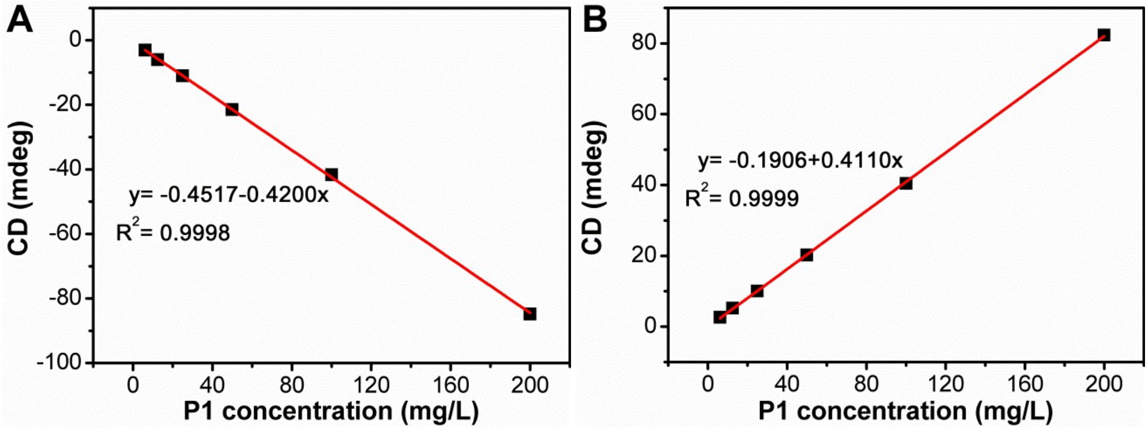

**Figure S5.** The plot of the CD intensity (at 437 nm) of HG−CM structures containing M2(R) (A) or M2(S) (B) as a function of P1 concentration.

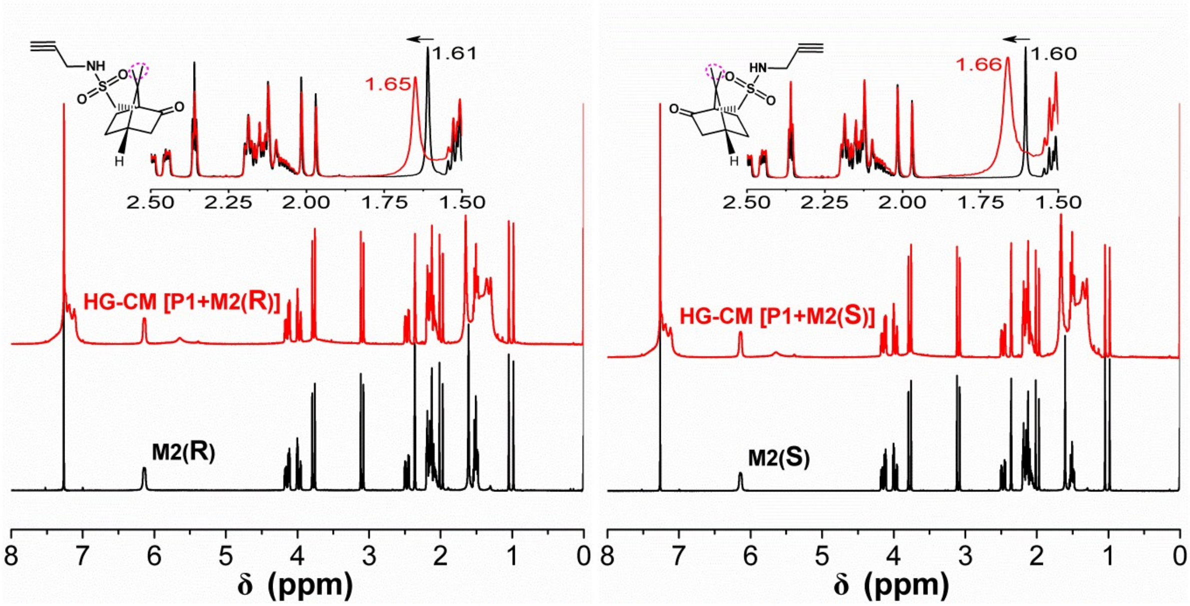

**Figure S6.** $^1$H NMR spectra of M2 (dissolved in $CDCl_3$) and HG−CM structures (prepared using $CDCl_3$ as solvent). All the spectra were recorded at 298 K.

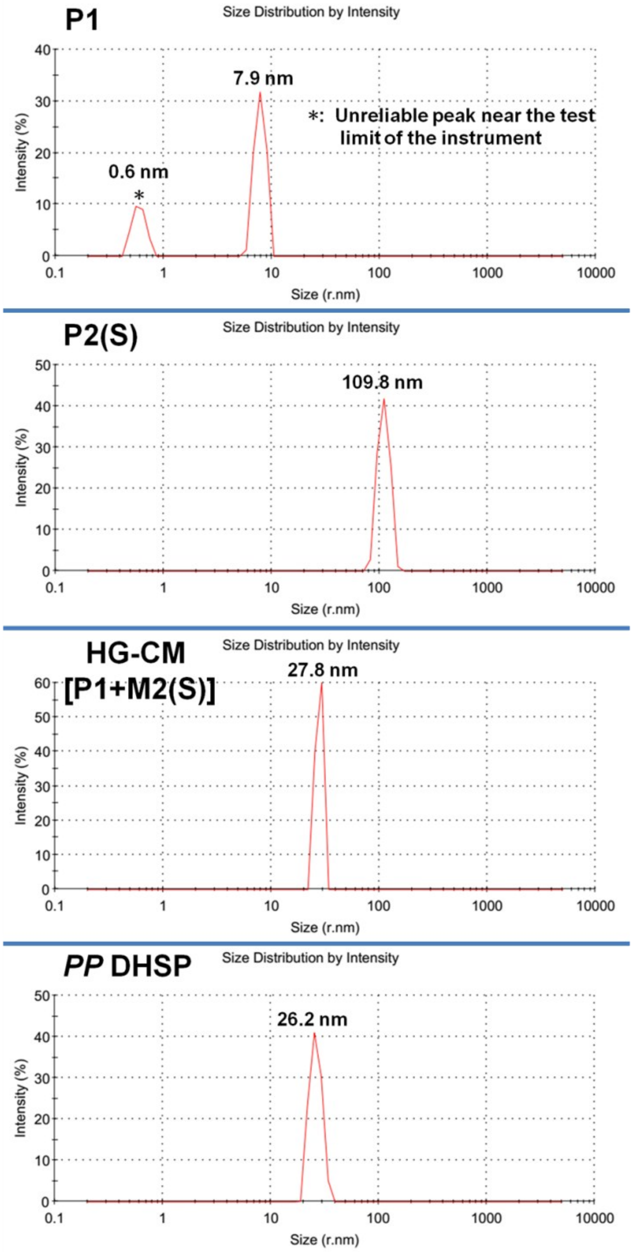

**Figure S7.** Hydrodynamic size of P1, P2(S), HG−CM [P1+M2(S)], and *PP* DHSP measured by dynamic light scattering (DLS) experiments. The samples were dissolved in $CHCl_3$ for the test, and all the tested solutions were completely transparent to the naked eye. The model for the calculation of hydrodynamic sizes is spherical, but the tested polymers are obviously not spherical. Therefore, the absolute value of the hydrodynamic sizes measured by DLS is not reliable, and thus we can only analyze the relative size of the polymers.

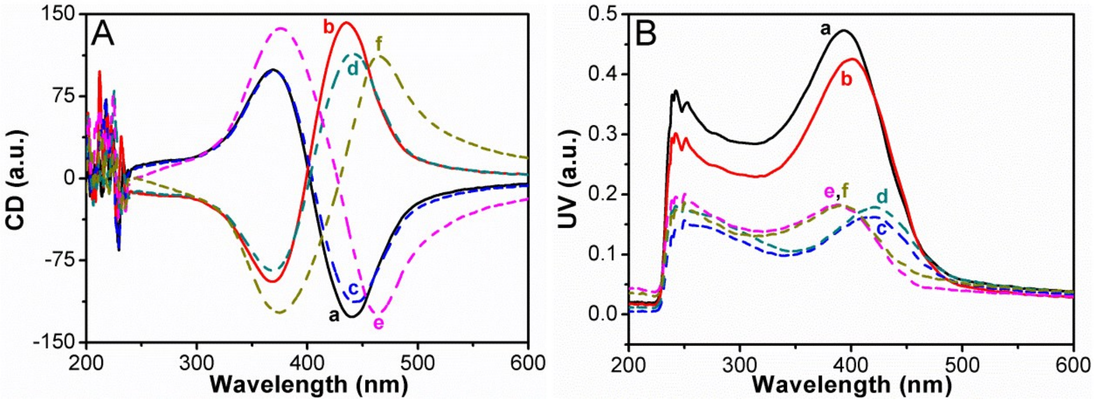

**Figure S8.** CD (A) and UV-vis (B) spectra of (a) a diluted $CHCl_3$ solution of the mixture of P1 and P2(R) in identical molar amount ([M1] = [M2(R)]); (b) a diluted $CHCl_3$ solution of the mixture of P1 and P2(S) in identical molar amount ([M1] = [M2(S)]); (c) P2(R) (0.01 mg/mL in $CHCl_3$); (d) P2(S) (0.01 mg/mL in $CHCl_3$); (e) the as-prepared *MM* DHSP (0.01 mg/mL in $CHCl_3$); and (f) the as-prepared *PP* DHSP (0.01 mg/mL in $CHCl_3$).

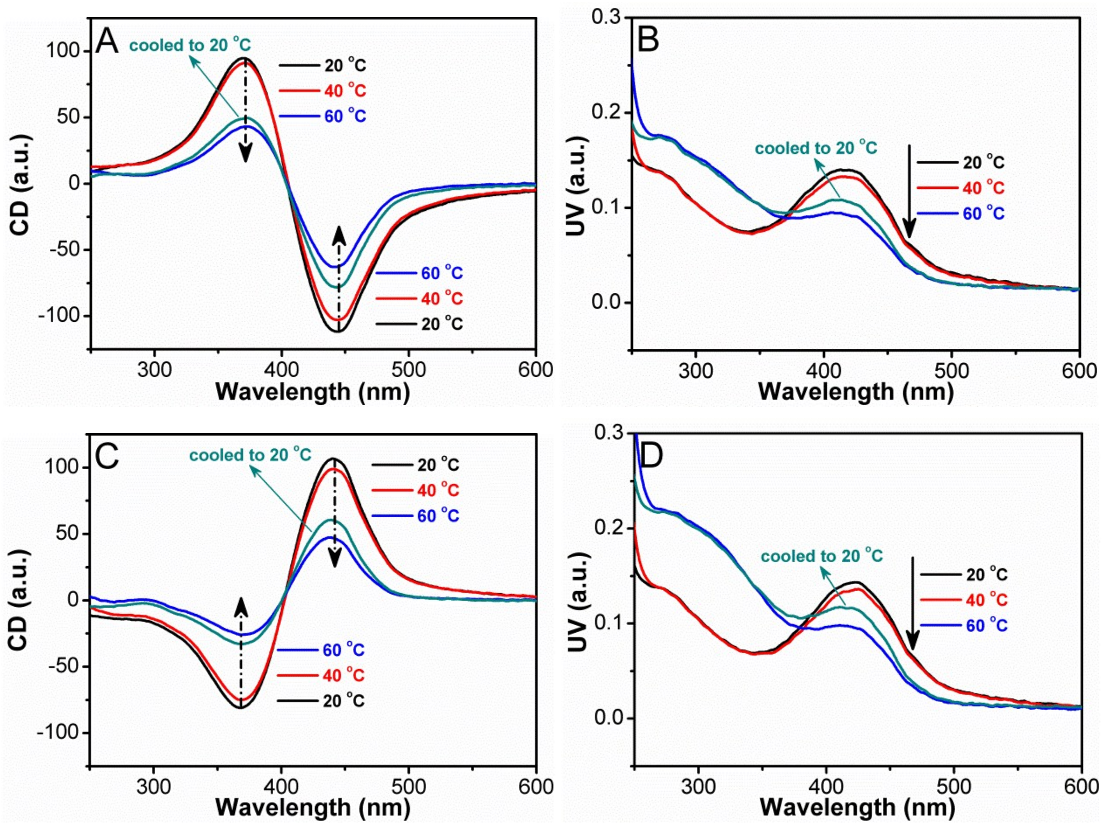

**Figure S9.** CD (A, C) and UV-vis (B, D) spectra of P2(R) (A, B) and P2(S) (C, D) dissolved in $CHCl_3$ at varied temperature: increased from 20 to 60 °C and then cooled to 20 °C again.

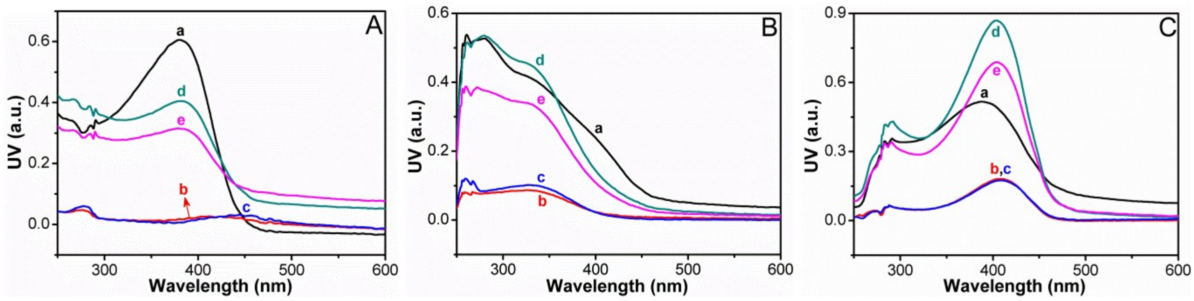

**Figure S10.** UV-vis spectra of (a) P1 (0.05 mg/mL), (b) P2(R) (0.01 mg/mL), (c) P2(S) (0.01 mg/mL), (d) *MM* DHSP (0.05 mg/mL), and (e) *PP* DHSP (0.05 mg/mL), measured in THF (A), DMSO (B), and toluene (C).

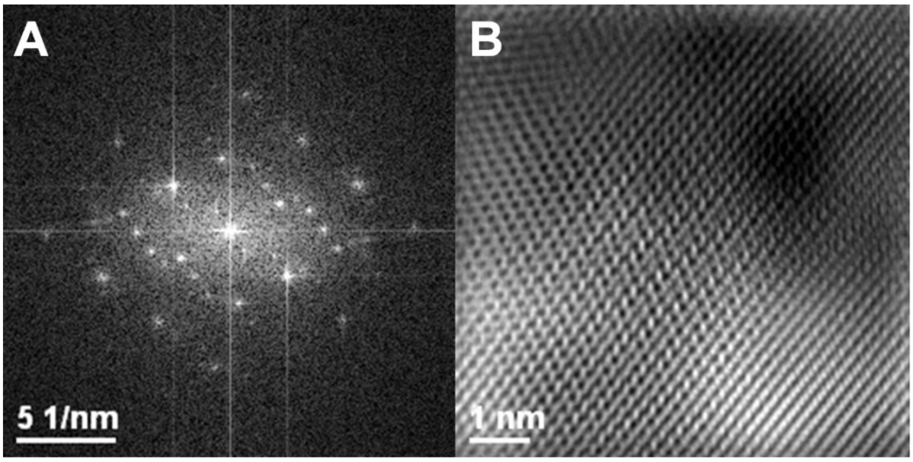

**Figure S11.** The selected area FFT image (A) and the corresponding filtered IFFT image (B) of *MM* DHSP.

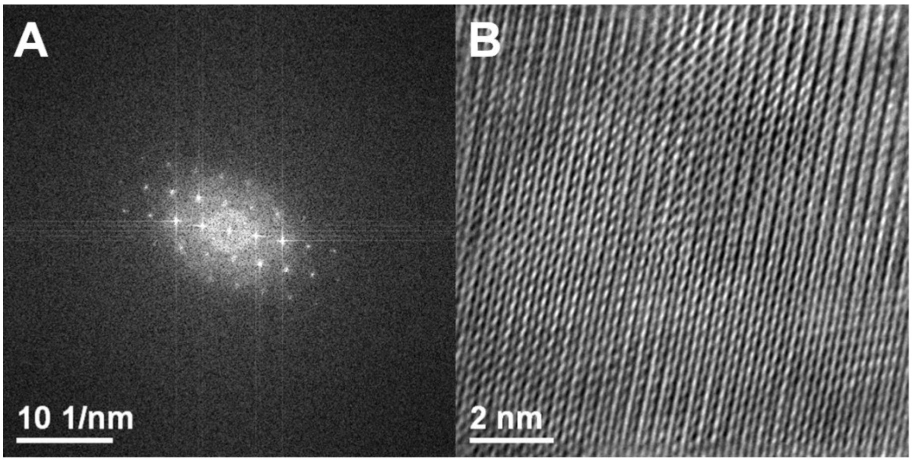

**Figure S12.** The selected area FFT image (A) and the corresponding filtered IFFT image (B) of *PP* DHSP.

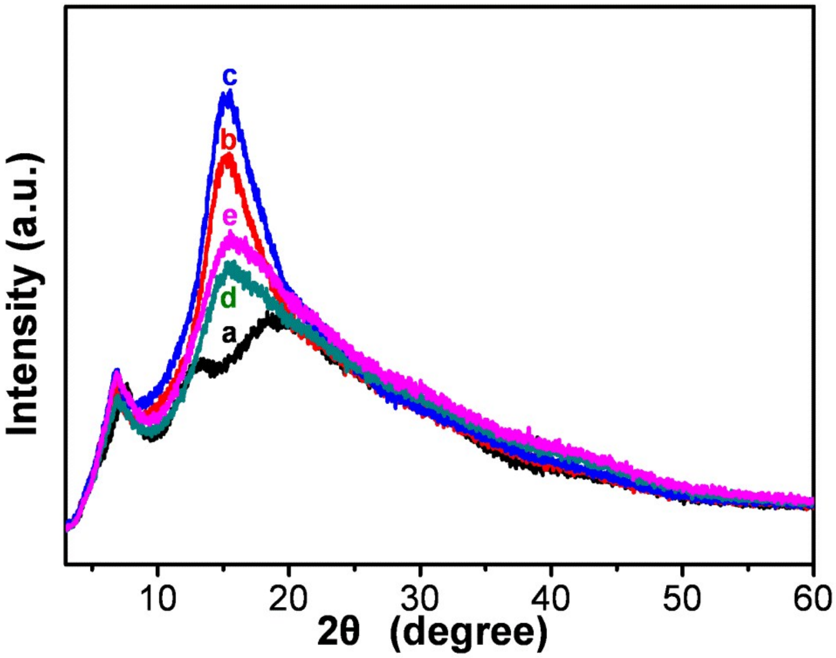

**Figure S13.** X-ray diffraction (XRD) spectra of (a) P1, (b) P2(R), (c) P2(S), (d) *MM* DHSP, and (e) *PP* DHSP.

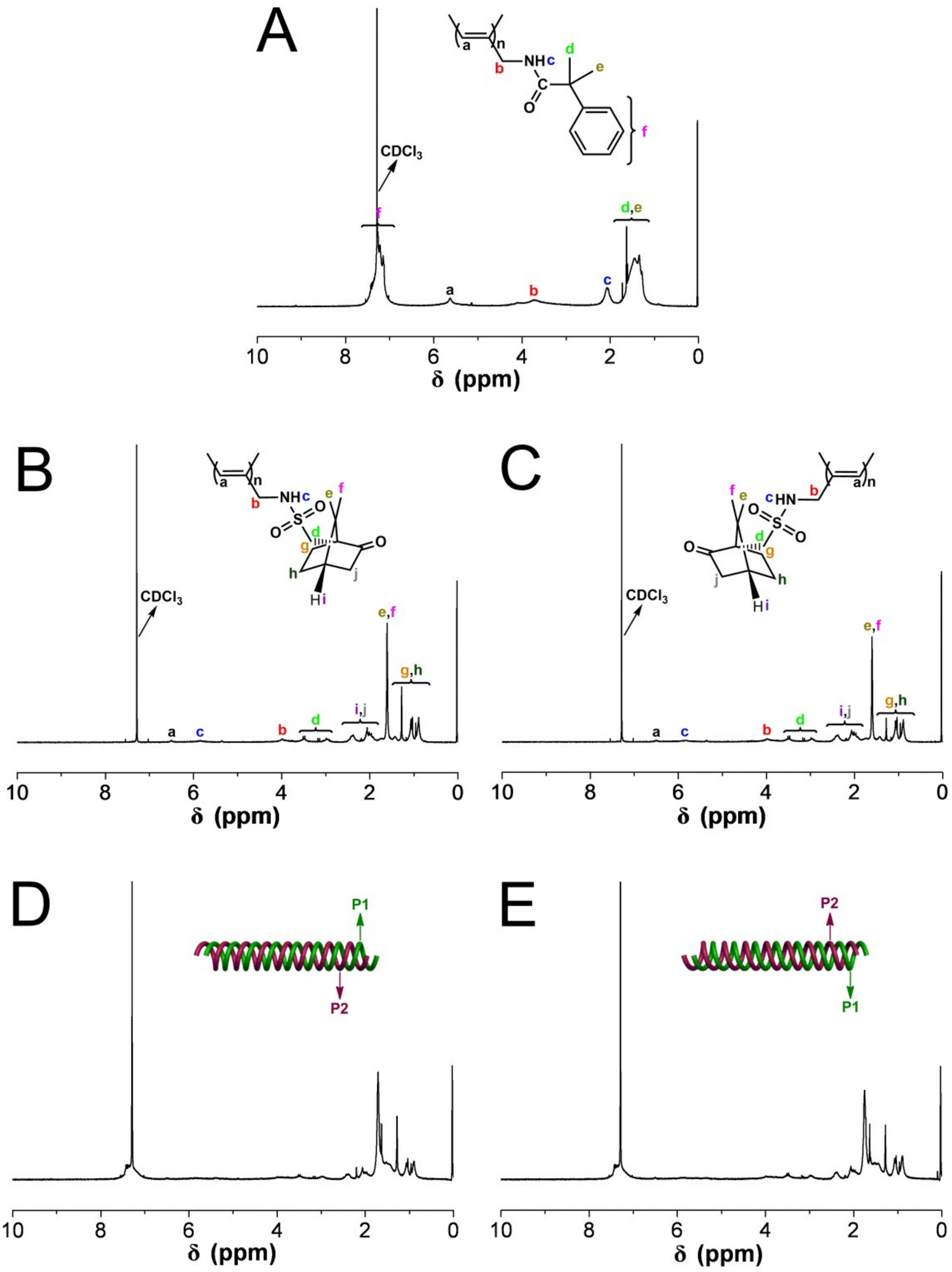

**Figure S14.** $^1$H NMR spectra (measured in $CDCl_3$, 298 K) of (A) P1, (B) P2(R), (C) P2(S), (D) *MM* DHSP, and (E) *PP* DHSP. All the samples were stored in a dryer before the measurement, thus the intense single-peak above 1.60 ppm observed in B−E should be assigned to the methyl groups in P2 instead of $H_2O$. The ratios of integral area of the thus-assigned peaks are consistent with the chemical structure of the corresponding product.

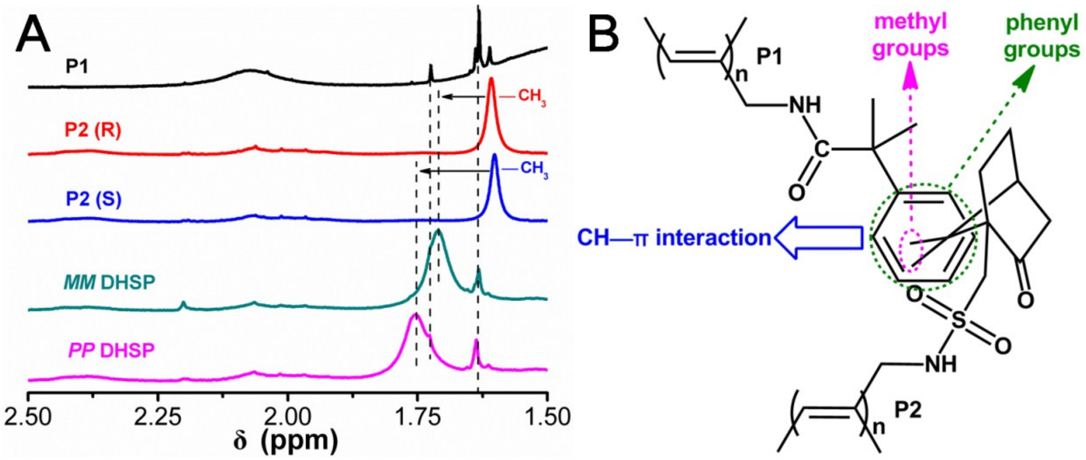

**Figure S15.** (A) Partial $^{1}$H NMR spectra of P1, P2(R), P2(S), *MM* DHSP, and *PP* DHSP. (B) The possible interaction between P1 and P2 in the DHSPs according to the information presented in (A).

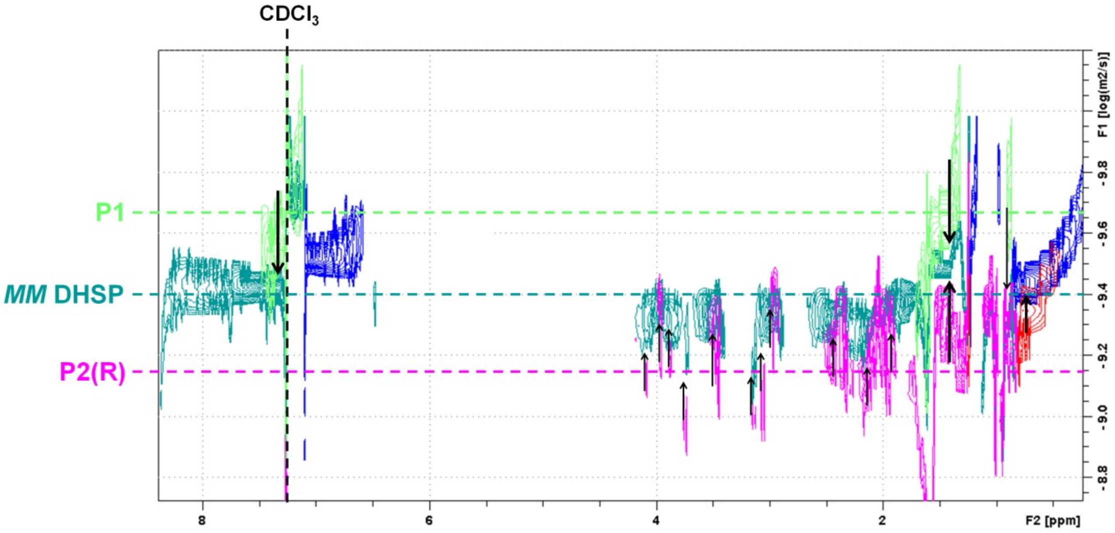

**Figure S16.** A comparison among the 2D $^{1}$H-DOSY NMR spectra of P1 (light green marks), P2(R) (pink and red marks), and *MM* DHSP (dark green and blue marks). As highlighted by black arrows, the diffusion coefficients of individual P1 and P2(R) were quite different, but the diffusion coefficients of P1 and P2(R) combined within *MM* DHSP became extremely close. All the samples were tested in the same condition (298 K, $CDCl_3$).

Some of the protons in relatively low content were not observed in the spectra due to their ***broad peaks*** (Figure S11) and the ***low solubility*** of the solid samples. The recorded signals were rather wide along the F1 axis because of the ***molecular weight distribution*** of the polymers.

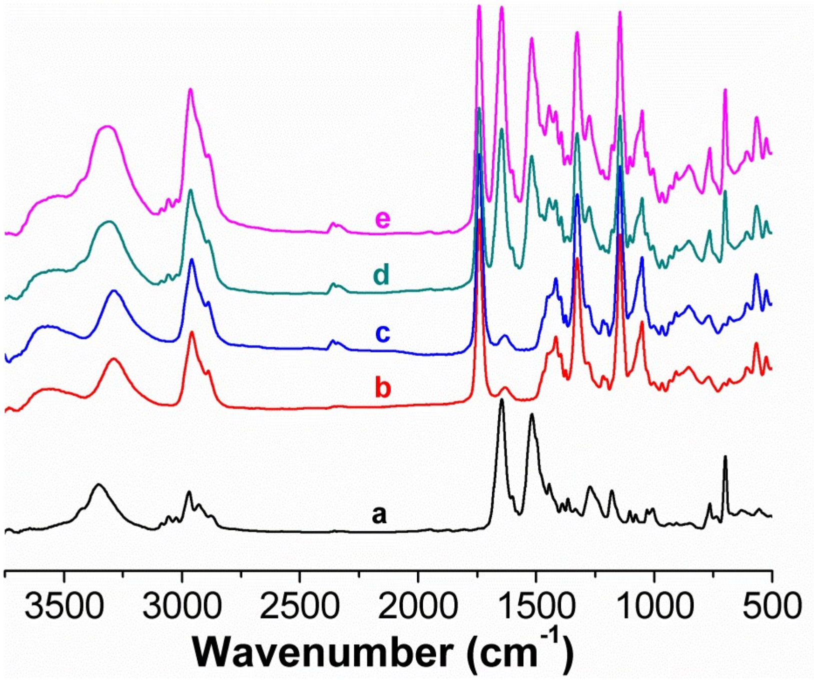

**Figure S17.** FT-IR spectra of (a) P1, (b) P2(R), (c) P2(S), (d) *MM* DHSP, and (e) *PP* DHSP.